

# High Methane Emissions from a Midlatitude Reservoir Draining an Agricultural Watershed

Jake J. Beaulieu,<sup>\*,†</sup> Rebecca L. Smolenski,<sup>†,‡,#</sup> Christopher T. Nietch,<sup>†</sup> Amy Townsend-Small,<sup>‡,§</sup> and Michael S. Elovitz<sup>†</sup>

<sup>†</sup>United States Environmental Protection Agency, Office of Research and Development, National Risk Management Research Laboratory, Cincinnati, Ohio 45268, United States

<sup>‡</sup>Department of Geology, University of Cincinnati, Cincinnati, Ohio 45221, United States

<sup>§</sup>Department of Geography, University of Cincinnati, Cincinnati, Ohio 45221, United States

**S** Supporting Information



**ABSTRACT:** Reservoirs are a globally significant source of methane (CH<sub>4</sub>), although most measurements have been made in tropical and boreal systems draining undeveloped watersheds. To assess the magnitude of CH<sub>4</sub> emissions from reservoirs in midlatitude agricultural regions, we measured CH<sub>4</sub> and carbon dioxide (CO<sub>2</sub>) emission rates from William H. Harsha Lake (Ohio, U.S.A.), an agricultural impacted reservoir, over a 13 month period. The reservoir was a strong source of CH<sub>4</sub> throughout the year, emitting on average  $176 \pm 36 \text{ mg C m}^{-2} \text{ d}^{-1}$ , the highest reservoir CH<sub>4</sub> emissions profile documented in the United States to date. Contrary to our initial hypothesis, the largest CH<sub>4</sub> emissions were during summer stratified conditions, not during fall turnover. The river–reservoir transition zone emitted CH<sub>4</sub> at rates an order of magnitude higher than the rest of the reservoir, and total carbon emissions (i.e., CH<sub>4</sub> + CO<sub>2</sub>) were also greater at the transition zone, indicating that the river delta supported greater carbon mineralization rates than elsewhere. Midlatitude agricultural impacted reservoirs may be a larger source of CH<sub>4</sub> to the atmosphere than currently recognized, particularly if river deltas are consistent CH<sub>4</sub> hot spots. We estimate that CH<sub>4</sub> emissions from agricultural reservoirs could be a significant component of anthropogenic CH<sub>4</sub> emissions in the U.S.A.

## INTRODUCTION

Methane (CH<sub>4</sub>) is a potent greenhouse gas (GHG) with a heat trapping capacity 34 times greater than that of carbon dioxide (CO<sub>2</sub>) on a 100 year time scale.<sup>1</sup> Human activities have more than doubled atmospheric CH<sub>4</sub> concentrations since the preindustrial era and current levels are unprecedented in at least the last 650 000 years. Known anthropogenic sources of CH<sub>4</sub> include livestock production, rice agriculture, landfills, and natural gas mining,<sup>2</sup> but current inventories may underestimate CH<sub>4</sub> emissions in the United States,<sup>3</sup> suggesting that additional sources may exist.

An important source of CH<sub>4</sub> is microbial activity in the sediments of aquatic ecosystems. Methane can be transported from sediments via gas bubble ebullition, molecular diffusion, or advection through plant stems.<sup>4</sup> Ebullition and plant stems can be important transport mechanisms in shallow waters and wetlands, but diffusion is typically the dominant evasion

pathway in deeper waters. Methane can also be oxidized to CO<sub>2</sub> via methanotrophic bacteria in areas where dissolved CH<sub>4</sub> and oxygen co-occur.<sup>4</sup>

The evasion of CH<sub>4</sub> to the atmosphere from the surfaces of reservoirs constructed for hydropower and other purposes may account for up to 20% of the global anthropogenic budget,<sup>5</sup> but these estimates are largely based on measurements made in undeveloped watersheds in tropical and boreal regions. Relatively little is known about emission rates from midlatitude systems, although ~30% of all reservoirs are located in this region.<sup>6</sup> Global estimates assume that reservoir CH<sub>4</sub> emissions decrease exponentially from the tropics to boreal regions, a

**Received:** April 17, 2014

**Revised:** July 3, 2014

**Accepted:** August 26, 2014

**Published:** August 26, 2014

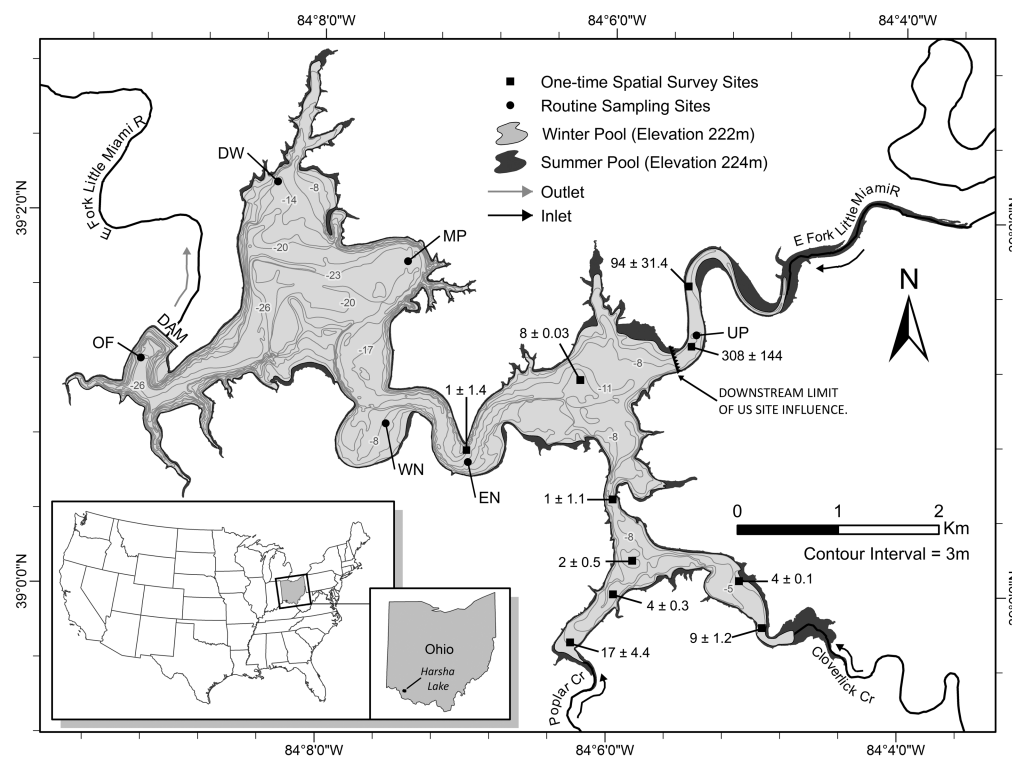


**Figure 1.** William H. Harsha Lake (Harsha Lake), tributaries, outlet, routine sampling sites, and one-time spatial survey sites. The different pool elevations reflect the change in surface area between the summer and winter pool elevations (224 m and 222 m, respectively). The area upstream of the line labeled ‘downstream limit of UP site influence’, was used to calculate the portion of the reservoir defined as having a methane ( $\text{CH}_4$ ) emission rate equal to that measured at UP. Results of the  $\text{CH}_4$  emission rates ( $\pm$  SE,  $\text{mg C m}^{-2} \text{d}^{-1}$ ) measured during the one-time spatial survey, completed on 8 January 2013 in the eastern portion of the reservoir, are reported adjacent to each sampling point as a mean  $\pm$  SE.

pattern that is largely attributed to differences in temperature.<sup>6</sup> A few studies of midlatitude systems support this pattern;<sup>7</sup> however, local scale characteristics, such as watershed land use or reservoir morphology, may cause  $\text{CH}_4$  emissions to deviate from this pattern.

Microbial respiration in oxic sediments mainly produces  $\text{CO}_2$ , but under anoxic conditions, respiration can also produce  $\text{CH}_4$ . Impounding river networks promotes sediment anoxia, and this may be particularly true for midlatitude agricultural impacted reservoirs that are subject to high nutrient and sediment loading rates. Watershed soil erosion can stimulate  $\text{CH}_4$  production by providing microbial communities with a large source of carbon (C) that can deplete sediment oxygen and fuel  $\text{CH}_4$  production. Algal blooms from excessive nutrient loading can further enrich reservoir sediments with labile C.<sup>9</sup> These factors may result in  $\text{CH}_4$  emission rates that are much higher than predicted from the generalized relationship between latitude and  $\text{CH}_4$  emissions.<sup>6</sup> However, low rates of methanogenesis during winter may balance high  $\text{CH}_4$  emission rates during the summer months, complicating efforts to predict the magnitude of  $\text{CH}_4$  emissions from midlatitude reservoirs.

To assess the possible importance of agricultural impacted reservoirs in the U.S. anthropogenic  $\text{CH}_4$  budget, we constructed an annual  $\text{CH}_4$  budget for William H. Harsha Lake, a eutrophic, seasonally stratified reservoir in southwestern Ohio (U.S.A.). Methane and  $\text{CO}_2$  emissions were measured approximately monthly in six locations throughout the lake using floating chambers, with increased sampling frequency in fall to assess the importance of  $\text{CH}_4$  release during the

ventilation of hypolimnetic waters. We combined the measurements with a conservative estimate of the areal extent of agricultural impacted reservoirs in the United States to produce a national scale estimate of  $\text{CH}_4$  emissions from agricultural reservoirs.

## MATERIALS AND METHODS

**Study Site.** William H Harsha Lake (hereafter referred to as Harsha Lake) is a 8.74  $\text{km}^2$  flood control reservoir built in 1978 on the East Fork Little Miami River in southwestern Ohio (U.S.A.) (Figure 1). The dam control structure allows for water withdrawal depths ranging from near the sediment–water interface to 3 m below the water surface. The reservoir is located within a state park, where it supports a recreational fishery, swimming beaches, and drinking water withdrawals. This warm monomictic reservoir ranges from ca. 4 m deep at the most upstream portions to 30 m near the dam and has a storage volume of  $111 \times 10^6$  and  $101.3 \times 10^6 \text{ m}^3$  at the summer and winter pool elevations, respectively. Mean outflows from the reservoir are  $78 \times 10^3$  and  $369 \times 10^3 \text{ m}^3 \text{ day}^{-1}$  at summer and winter pool elevations, respectively, corresponding to mean water residence times of 1424 and 274 days. The reservoir receives substantial nutrient and sediment loading from the watershed (64% row crop agriculture) and is frequently on the state’s advisory list for recreational contact due to excessive blue-green algae (<http://epa.ohio.gov/habalgae.aspx>).

Six sites (upstream (UP), east narrows (EN), west narrows (WN), midpoint (MP), drinking water intake (DW), and out-fall (OF)) were established to characterize spatial patterns in  $\text{CH}_4$  and  $\text{CO}_2$  dynamics. Sampling began in October 2011 and

continued on a monthly basis until June 2012, when the frequency was increased to every 3 weeks. Sampling frequency was further increased to weekly from October 2012 to November 2012 to better characterize emissions during fall turnover, defined as the period between when thermal stratification begins to degrade and isothermal conditions are achieved.

On 08 January 2013, we measured CH<sub>4</sub> emission rates from two of the routine sampling sites (UP and EN) and an additional 8 sites in the upstream reaches of the reservoir (Figure 1). The objective of this sampling was to determine if bays with tributaries had higher CH<sub>4</sub> emission rates than open water sites.

**Water Sample Collection.** Water samples were collected for dissolved CH<sub>4</sub> analysis from 0.1 m below the surface and 1 m above the sediment at all sites. During summer stratification (9 May 2012 to 24 Oct 2012) additional samples were collected at 5 m increments throughout the water column at the OF site. At least 10% of the samples were collected in duplicate. Water samples were collected in 125 mL serum bottles and preserved with 1000 μL of saturated mercuric chloride solution. Bottles were capped with gray butyl rubber septa and stored at 5 °C until sample analysis. During the summer of 2013 (24 July, 27 August) seven water samples were collected from throughout the water column at the OF site and analyzed for CH<sub>4</sub> concentration and δ<sup>13</sup>C—CH<sub>4</sub>.

We extracted dissolved gases from the water samples using headspace equilibration.<sup>10</sup> The headspace equilibration was conducted at room temperature by injecting 20 mL of ultra high purity dinitrogen (N<sub>2</sub>) into the sample serum vial, while allowing an equivalent volume of water to be displaced from the bottle through a vent needle. The water bottles were then shaken for at least 1 h before the headspace was analyzed. The original dissolved gas concentration was calculated using the measured headspace gas concentration and temperature specific Bunsen solubility coefficients.<sup>11,12</sup> Equilibrium dissolved CH<sub>4</sub> concentrations were calculated for each sampling date using water temperature, barometric pressure, and their average global atmospheric concentration.<sup>13</sup> Dissolved gas saturation ratio was calculated as the ratio of measured to equilibrium dissolved gas concentrations.

We measured water temperature and dissolved oxygen using a data sonde (YSI 600 OMS, Yellow Springs, Ohio, U.S.A.) at each depth where a water sample was collected. Atmospheric pressure was measured using an electronic barometer on each sampling date (YSI 650 MDS, Yellow Springs, OH, U.S.A.). We measured CH<sub>4</sub> and CO<sub>2</sub> using a Shimadzu GC-2014 (Kyoto, Japan) or Bruker 450 (Billerica, MA, U.S.A.) gas chromatograph equipped with a methanizer and flame ionization detector (FID) (additional details in the extended methods section in the SI). Methane δ<sup>13</sup>C—CH<sub>4</sub> was measured at the University of California Davis Stable Isotope Facility.<sup>14</sup>

**CH<sub>4</sub> and CO<sub>2</sub> Emissions.** Methane and CO<sub>2</sub> emission rates were measured using the floating chamber technique, as previously described.<sup>15</sup> At each of the six sites, three 20 L acrylic chambers were supported by air filled flotation collars, tethered to the boat, and allowed to drift with the boat. Gas samples (30 mL) were withdrawn from the chamber headspace every 3 min for 12 min and stored in pre-evacuated glass vials. Emission rates were computed from the linear regression of headspace CH<sub>4</sub> or CO<sub>2</sub> partial pressure against time, after accounting for the headspace volume and surface area of the reservoir enclosed by the chamber. Emission rates were only

calculated for chambers where the linear regression was significant at the  $p < 0.15$  level (see Supporting Information, SI, Methods).

The piston velocity ( $k$ ; cm hr<sup>-1</sup>) describes the physical forcing component of air–water gas exchange and can indicate whether rising bubbles or diffusive emissions were captured by the floating chambers. We calculated  $k$  from the CH<sub>4</sub> and CO<sub>2</sub> data for each chamber deployment according to the following:

$$k = \text{emission rate} / [C_w - C_{eq}] \quad (1)$$

where  $C_w$  (mg C m<sup>-3</sup>) and  $C_{eq}$  (mg C m<sup>-3</sup>) are the measured and equilibrium dissolved gas concentrations near the water surface (10 cm).<sup>15</sup> If the emissions were purely diffusive, then piston velocities calculated from CH<sub>4</sub> and CO<sub>2</sub> should be identical when normalized to a Schmidt number of 600 ( $k_{600}$ ). Values of  $k_{600\text{-CH}_4}$  that far exceed those of  $k_{600\text{-CO}_2}$  can occur when the chambers capture CH<sub>4</sub> rich bubbles and were used as an indicator of ebullition (see SI Extended Methods).

We calculated average reservoir-wide CH<sub>4</sub> emission rates for each sampling date as follows:

$$\text{Reservoir wide emission rate} = \sum E_i P_i \quad (2)$$

where  $E_i$  and  $P_i$  are the measured emission rate and proportion of the reservoir surface area associated with site  $i$ , respectively. The reservoir surface area associated with the UP site was defined as extending from the upstream extent of the impounded waters along the East Fork Little Miami River, the main tributary, downstream to the area where the reservoir widens and the depth reaches 8 m (Figure 1). This boundary was selected based on the spatial survey conducted in the fall of 2012. The other five routine sampling sites were weighted equally, because there was no significant difference in emission rates between these sites.

Reservoir-wide CH<sub>4</sub> emissions were estimated for each day of the study by assuming the emission rate on days between sampling events was equal to the emission rate measured on the closest sampling date, and multiplying the reservoir-wide rate by the reservoir surface area. Daily reservoir surface area was calculated from the reported elevation of the water surface and 0.3 m resolution elevation data (0.58 m<sup>2</sup> grid size) using a geographic information system (ESRI, Redlands, California, U.S.A.). An annual reservoir-wide CH<sub>4</sub> emission rate was calculated by summing the daily emissions across the year and normalizing them to the mean annual reservoir surface area.

The standard deviation of the reservoir-wide annual CH<sub>4</sub> emission rate was calculated as the average coefficient of variation (CV) of the replicate emission rate measurements made at each site and date, multiplied by the estimated reservoir-wide annual emission rate (i.e., standard deviation = CV\*mean). Standard error was calculated by dividing the standard deviation by the square root of the number of sampling dates.

We estimated the total surface area of agricultural impacted reservoirs in the U.S.A. using data from the National Inventory of Dams<sup>16</sup> and agricultural statistics from the National Agricultural Statistics Service.<sup>17</sup> All reservoirs located in counties with greater than 40 km<sup>2</sup> of corn and soybean were defined as agricultural. This approach does not account for reservoirs affected by other types of agricultural activities, including pastures and confined animal feed lots that could deliver nutrients and sediments to reservoirs.

**CH<sub>4</sub> Degassing.** We estimated CH<sub>4</sub> degassing as water passed through the dam as the product of daily depth-specific withdrawal rates (provided by the U.S. Army Corps of Engineers) and the dissolved CH<sub>4</sub> concentration at the depth from which



water was being withdrawn. We used measured  $\text{CH}_4$  concentrations at the “OF” site which was located ca. 150 m from the withdrawal structure. Linear interpolation was used to extrapolate  $\text{CH}_4$  concentration between sampling depths. For dates when dissolved  $\text{CH}_4$  was not measured, the  $\text{CH}_4$  concentration from the nearest sampling date was used. We assumed that all dissolved  $\text{CH}_4$  was emitted (degassed) during transit through the outlet structure or further downstream.

**Hypolimnion  $\text{CH}_4$  Accumulation, Oxidation, Diffusion, And Production.** We estimated the hypolimnion  $\text{CH}_4$  production rate ( $\text{MP}_{\text{hypo}}$ ) at the OF site during the period of stratification as the sum of hypolimnion  $\text{CH}_4$  accumulation ( $\text{MA}_{\text{hypo}}$ ), hypolimnion  $\text{CH}_4$  oxidation ( $\text{MOX}_{\text{hypo}}$ ), and  $\text{CH}_4$  diffusion from the hypolimnion into the epilimnion ( $\text{MD}_{\text{hypo}}$ ). Detailed descriptions of the calculations can be found in the SI Extended Methods. The hypolimnion  $\text{CH}_4$  accumulation rate was calculated from the depth profiles of  $\text{CH}_4$  concentration during stratification as previously described.<sup>18</sup> The fraction of  $\text{CH}_4$  entering the hypolimnion that was oxidized ( $f_{\text{ox}}$ ) was estimated from the  $\delta^{13}\text{C}-\text{CH}_4$  depth profiles at the OF site using an open-system steady-state model.<sup>19,20</sup> The rate of  $\text{CH}_4$  oxidation in the hypolimnion was calculated as follows:

$$\text{MOX}_{\text{hypo}} = f_{\text{ox}} \times \text{MA}_{\text{hypo}} \quad (3)$$

Methane diffusion across the thermocline from the hypolimnion ( $\text{MD}_{\text{hypo}}$ ) was calculated from the vertical diffusion coefficient ( $K$ ,  $\text{m}^2 \text{d}^{-1}$ ) and the  $\text{CH}_4$  concentration gradient between the top of the hypolimnion and the epilimnion.<sup>21</sup>

**Statistics.** We used generalized least-squares (gls) to test for differences in emission rates among sampling sites and to test for a relationship between  $\text{CH}_4$  emission rates and water temperature. Heterogeneity in model residuals was reduced by adding variance covariates.<sup>22</sup> We tested for temporal autocorrelation by comparing the Akaike’s information criterion (AIC)<sup>23</sup> of models with and without a first-order autoregressive (AR1) temporal correlation structure.<sup>22</sup> The model with the lowest AIC was retained. When emission rates were found to differ by site, pairwise comparisons were made using the Tukey’s test. All statistical analysis were conducted using R.<sup>24</sup> The gls models were built with the nlme package<sup>25</sup> and Tukey’s tests were conducted using the multcomp package.<sup>26</sup>

## RESULTS

### Hydrology, Water Temperature, and Dissolved Oxygen.

Reservoir water levels were close to the management targets of 222.3 and 223.5 m during the winter and summer, respectively (SI Figure S1). Water levels were dropped to 221 m in April 2012 before the reservoir was filled to the summer management target. Water levels transitioned between the seasonal management targets during fall and were temporarily elevated following precipitation events during the winter and spring. The water column was isothermal from 6 Dec 2011 to 9 May 2012, and some degree of thermal stratification was observed during the balance of the study (SI Figure S2A). The water column was oxygenated until the onset of thermal stratification, when the dissolved oxygen (DO) saturation fell to 0.2–3.8% in the hypolimnion, but remained above 100% in the epilimnion (SI Figure S2B). During fall turnover, DO was approximately 30% saturated throughout the water column.

**Piston Velocities.** The median gas piston velocities ( $k_{600}$  in  $\text{cm h}^{-1}$ ) were 4.2 and 27.2 for  $\text{CO}_2$  and  $\text{CH}_4$ , respectively (Figure 2). In the 97 instances where  $k_{600-\text{CH}_4}$  and  $k_{600-\text{CO}_2}$  were

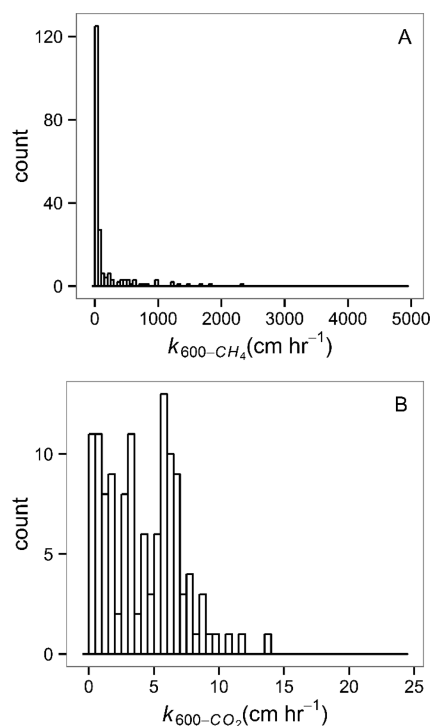


**Figure 2.** Histogram of (A) piston velocities calculated from dissolved  $\text{CH}_4$  concentration and  $\text{CH}_4$  emission rates ( $k_{600-\text{CH}_4}$ ), and (B) piston velocities calculated from dissolved  $\text{CO}_2$  concentration and  $\text{CO}_2$  emission rates ( $k_{600-\text{CO}_2}$ ). Panels A and B have binwidths of 50 and 0.5, respectively.

measured in the same chamber (see the SI Methods for data acceptance criteria),  $k_{600-\text{CH}_4}$  was a median factor of 21 times greater than  $k_{600-\text{CO}_2}$ , suggesting that the chambers intercepted  $\text{CH}_4$  rich bubbles rising to the water surface. The difference between the  $\text{CH}_4$  and  $\text{CO}_2$   $k_{600}$  values was most extreme at the shallowest sites (EN and UP) ( $p < 0.005$ ).

**Methane and Carbon Dioxide.** Methane was supersaturated with respect to atmospheric equilibrium throughout the study (SI Table S1). Methane concentration ranged from 0.16 to 250  $\mu\text{g CH}_4 \text{L}^{-1}$  in the epilimnion (saturation ratio of 3 to 6800), highest in summer and lowest in the winter (Figure 3). Hypolimnion  $\text{CH}_4$  concentration increased exponentially from the thermocline to the sediment–water interface during stratification at the deepest site (OF), reaching a maximum value of 18 500  $\mu\text{g CH}_4 \text{L}^{-1}$  (saturation ratio = 374 700) on 24 Oct 2012 (Figure 4). Differences in  $\text{CH}_4$  concentration between shallow and deep waters declined with overall site depth and no consistent difference was observed at the shallowest site (UP). See the SI Extended Methods for QA/QC data.

On 24 July and 27 August 2013,  $\delta^{13}\text{CCH}_4$  near the sediment water interface at the OF site ranged from  $-63.4$  to  $-61.8\text{‰}$  and increased to  $-57.5\text{‰}$  at the top of the hypolimnion (SI Figure S3), equating to  $f_{\text{ox}}$  values of 0.29 and 0.23, respectively. We therefore assumed an  $f_{\text{ox}}$  value of 0.25 during the period of thermal stratification in 2012. Hypolimnion  $\text{CH}_4$  accumulation ( $\text{MA}_{\text{hypo}}$ ) rates at the OF site ranged from 719 to 1531  $\text{mg C m}^{-2} \text{d}^{-1}$  (median = 792) (Table 1). Hypolimnion  $\text{CH}_4$  oxidation ( $\text{MOX}_{\text{hypo}}$ ), calculated as the product of  $f_{\text{ox}}$  and  $\text{MA}_{\text{hypo}}$ , ranged from 180–383  $\text{mg C m}^{-2} \text{d}^{-1}$  (median = 198) (Table 1). Rates of  $\text{CH}_4$  diffusion across the thermocline ( $\text{MD}_{\text{hypo}}$ ) ranged from 6–106  $\text{mg C m}^{-2} \text{d}^{-1}$  and increased throughout the period of thermal stratification (Table 1; see SI

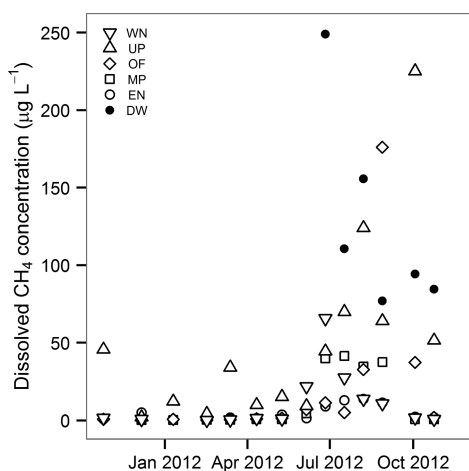


**Figure 3.** Dissolved methane (CH<sub>4</sub>) concentration at ~0.1m depth at the six sampling sites in Harsha Lake from 25 Oct 2011 to 24 Oct 2012.

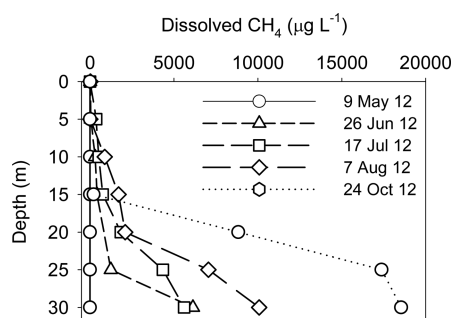


**Figure 4.** Depth profiles of dissolved methane concentration on given sampling dates at the OF site.

Table S1 for details). Hypolimnion CH<sub>4</sub> production (MP<sub>hypo</sub>) ranged from 908–1934 mg C m<sup>-2</sup> d<sup>-1</sup> (median = 1061) (Table 1).

Of 333 chamber deployments, 49 CH<sub>4</sub> and 30 CO<sub>2</sub> emission rate calculations resulted in regression models with *p* values greater than 0.15 and were assigned an emission rate of 0. The median coefficient of determination (*r*<sup>2</sup>) for the CH<sub>4</sub> and CO<sub>2</sub> regression models was 0.94 (range: 0.56–0.99) and 0.97 (range: 0.58–0.99), respectively (SI Figure S4). The mean daily CH<sub>4</sub> emission rate (±SE) at the most upstream site (UP) was 2353 ± 495 mg C m<sup>-2</sup> d<sup>-1</sup>, was one to 2 orders of magnitude greater than the other sites (*p* < 0.001; Figure 5A, SI Table S2). The CH<sub>4</sub> emission rates observed near the tributaries during the one-time spatial survey on 8 Jan 2013 were on average six times higher than EN, the open water site, but were an order

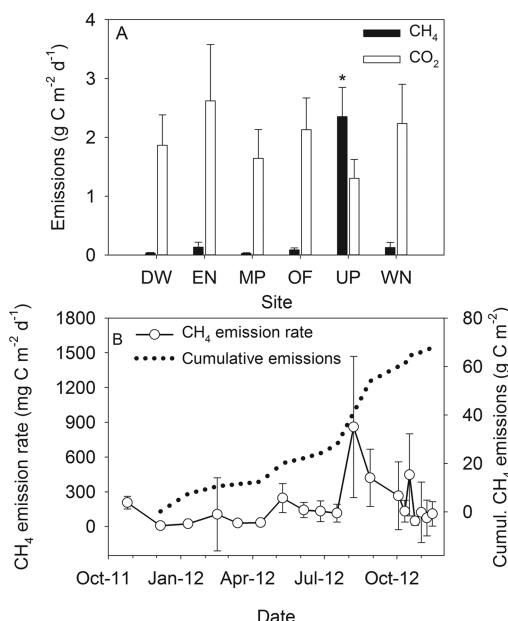


**Figure 5.** (A) Mean (+SE) methane (CH<sub>4</sub>) and carbon dioxide (CO<sub>2</sub>) emission rates at the 6 routine sampling sites. The star denotes that CH<sub>4</sub> emission rates at UP were significantly different than the other sites (*p* < 0.001). Methane emission rates did not differ among other sites. (B) Reservoir-wide CH<sub>4</sub> emission rates (±SE) on each sampling date (solid line, open circles, primary y-axis) and cumulative CH<sub>4</sub> emissions from 6 Dec 2011 through 15 Nov 2012 (dashed line, secondary y-axis).

of magnitude lower than at UP (rates reported alongside sampling sites in Figure 1). Methane emission rates increased by 3.5 mg C m<sup>-2</sup> d<sup>-1</sup> per degree increase in water temperature (*p* < 0.001, SI Figure S5). A linear model containing site and water temperature explained 47% of the variation in CH<sub>4</sub> emission rates.

The mean annual CO<sub>2</sub> emission rate was lowest at UP (1.3 ± 0.3 g C m<sup>-2</sup> d<sup>-1</sup>) and the rates among the other sites did not differ, *p* < 0.001 (Figure 5A, SI Table S2). Total carbon emissions (CO<sub>2</sub> + CH<sub>4</sub>), an index for total carbon mineralization, were greater at UP (mean ± SE: 3.7 ± 0.6 g C m<sup>-2</sup> d<sup>-1</sup>) than all other sites except EN (*p* < 0.001; mean ± SE of all sites excluding UP: 2.2 ± 0.3 g C m<sup>-2</sup> d<sup>-1</sup>) (Figure 5A). The proportion of mineralized C emitted as CH<sub>4</sub> was also greater at UP (0.60 ± 0.07) than all other sites (*p* < 0.001, mean ± SE of all sites excluding UP: 0.11 ± 0.05).

**Table 1.** Hypolimnion Methane (CH<sub>4</sub>) Accumulation, Oxidation, Trans-Thermocline Diffusion, And Production Rates Measured at the Deepest Site (OF) during the 2012 Period of Thermal Stratification

period	hypolimnion CH <sub>4</sub> accumulation (mg CH <sub>4</sub> -C m <sup>-2</sup> d <sup>-1</sup> )	hypolimnion CH <sub>4</sub> oxidation <sup>a</sup> (mg CH <sub>4</sub> -C m <sup>-2</sup> d <sup>-1</sup> )	trans-thermocline CH <sub>4</sub> diffusion <sup>b</sup> (mg CH <sub>4</sub> -C m <sup>-2</sup> d <sup>-1</sup> )	hypolimnion CH <sub>4</sub> production <sup>c</sup> (mg CH <sub>4</sub> -C m <sup>-2</sup> d <sup>-1</sup> )
05 Jun to 26 Jun	1409	352	6	1777
26 Jun to 17 Jul	719	180	9	908
17 Jul to 07 Aug	1531	383	21	1934
07 Aug to 28 Aug	792	198	35	1024
28 Aug to 03 Oct	764	190	106	1060

<sup>a</sup>Hypolimnion CH<sub>4</sub> oxidation calculated as the product of *f*<sub>ox</sub> and the hypolimnion CH<sub>4</sub> accumulation rate. We assigned a value of 0.25 to *f*<sub>ox</sub> based on δ<sup>13</sup>C-CH<sub>4</sub> data collected during the summer of 2013 (See SI Figure S3). <sup>b</sup>Methane diffusion is reported as the mean of the diffusion rates calculated for the first and last day of the measurement period. Positive values indicate net diffusion from hypolimnion into epilimnion. <sup>c</sup>Hypolimnion CH<sub>4</sub> production is calculated as the sum of hypolimnion CH<sub>4</sub> accumulation, oxidation, and trans-thermocline diffusion.

After accounting for spatial and temporal variability, we estimated the mean annual reservoir-wide  $\text{CH}_4$  emission rate as  $176 \pm 36 \text{ mg C m}^{-2} \text{ d}^{-1}$ . Reservoir wide  $\text{CH}_4$  emission rates were relatively low during the winter (mean daily emission rate =  $64 \text{ mg C m}^{-2} \text{ d}^{-1}$ , Figure 5B). Rates increased through the spring to a seasonal mean of  $117 \text{ mg C m}^{-2} \text{ d}^{-1}$  and reached a maximum of  $859 \text{ mg C m}^{-2} \text{ d}^{-1}$  during the warmest months. When the lake was undergoing fall turnover (11 Oct 2012–15 Nov 2012), the daily emission rates varied greatly ( $47\text{--}447 \text{ mg C m}^{-2} \text{ d}^{-1}$ ), but had a mean daily emission rate of  $157 \text{ mg C m}^{-2} \text{ d}^{-1}$ . Approximately half (51%) of the annual  $\text{CH}_4$  emissions occurred during the summer. Spring and fall accounted for 23% and 22% of annual emissions, respectively, while winter accounted for only 6%.

Release of  $\text{CH}_4$  to the atmosphere resulting from water passing through the dam control structure was a relatively small part of the annual  $\text{CH}_4$  budget. We estimate that an annual average of  $10.7 \text{ kg CH}_4\text{--C d}^{-1}$  was lost as the water degassed during transit through the Harsha Lake dam, equivalent to only 0.8% of the total emissions, or  $1.22 \text{ mg C m}^{-2} \text{ d}^{-1}$ .

## DISCUSSION

Harsha Lake was a consistent source of atmospheric  $\text{CH}_4$  throughout the year. Despite low  $\text{CH}_4$  emission rates during the winter months, average annual  $\text{CH}_4$  emissions were higher than previously reported for temperate reservoirs in the United States and comparable to those reported for tropical reservoirs.<sup>6</sup> The furthest upstream portions of the reservoir supported  $\text{CH}_4$  emissions one to 2 orders of magnitude greater than other portions of the system, highlighting the importance of including river deltas in reservoir  $\text{CH}_4$  budgets.

**$\text{CH}_4$  Emissions.** Seasonal patterns in  $\text{CH}_4$  emission rates were characterized by relatively low emissions during the winter months, maximum rates in the summer months, and small peaks superimposed on declining emissions during fall turnover (Figure 5B). Winter emissions were likely limited by low water temperature and greater  $\text{O}_2$  availability in bottom waters and sediments, which reduces the metabolic activity of methanogens.<sup>27</sup> The reservoir stratified during the warm summer months and  $\text{CH}_4$  progressively accumulated in the hypolimnion, reaching concentrations in excess of  $18\,000 \mu\text{g L}^{-1}$  (saturation ratio  $>300\,000$ ; Figure 4). Despite strong thermal stratification that prevented the advective transport of  $\text{CH}_4$  from the hypolimnion to the epilimnion, surface emissions also reached a maximum during late summer. Sources of  $\text{CH}_4$  to the air–water interface during periods of thermal stratification include diffusion from the hypolimnion,<sup>21</sup> lateral transport from the catchment<sup>28</sup> and littoral zone,<sup>29</sup> microbial  $\text{CH}_4$  production in the oxic epilimnion, and ebullition.<sup>30</sup> Rates of  $\text{CH}_4$  diffusion from the hypolimnion into the epilimnion were equivalent to a median of 44% (range: 6–481%) of the emission rate at OF during stratification, indicating that diffusion was, at times, an important source of  $\text{CH}_4$  to the epilimnion. Presumably lateral transport and oxic  $\text{CH}_4$  production accounted for the balance, and ebullition may contribute a significant portion of  $\text{CH}_4$  emissions, particularly at shallower sites (see below).

The thermocline progressively sank during fall turnover (SI Table S1, Figure S2A), causing hypolimnetic  $\text{CH}_4$  to mix into the epilimnion where it was either oxidized to  $\text{CO}_2$  or emitted to the atmosphere. We expected the greatest reservoir-wide emission rates to occur during turnover,<sup>31</sup> but the maximum emission rate during turnover ( $447 \text{ mg C m}^{-2} \text{ d}^{-1}$ )

was only half the highest rate observed during summer ( $860 \text{ mg C m}^{-2} \text{ d}^{-1}$ ), likely because cooler water temperatures during turnover depressed  $\text{CH}_4$  production at the shallow sites more than mixing enhanced  $\text{CH}_4$  emissions from the deeper sites. Despite the relatively low rates observed during turnover, 22% of annual  $\text{CH}_4$  emissions occurred during this time.<sup>32</sup>

Methane emission rates at the sampling site located near the delta at the river–reservoir transition zone (UP site) were consistently one to 2 orders of magnitude greater than the other sampling sites (Figure 5A). This site was typically the shallowest included in the study (mean depth = 4.25 m) and did not stratify during the summer. Shallow waters have been previously identified as  $\text{CH}_4$  emission hot spots in lakes and reservoirs<sup>4,29</sup> due partly to low water-column  $\text{CH}_4$  oxidation rates. The water residence time of  $\text{CH}_4$  in shallow waters is much less than in deeper waters, resulting in reduced methane oxidation efficiencies leading to an “epilimnetic shortcut”.<sup>4</sup> This scenario is supported by the high ratio of  $\text{CH}_4$  to  $\text{CO}_2$  emissions at the upstream site, which suggests that a larger fraction of the sedimentary  $\text{CH}_4$  is evading to the atmosphere, rather than being oxidized to  $\text{CO}_2$  (Figure 5A).

High rates of  $\text{CH}_4$  ebullition likely contributed to enhanced emissions at the UP site. Ebullition rates tend to be highest in shallow areas because short water residence times limit the dissolution of  $\text{CH}_4$  rich bubbles released from the sediment.<sup>33</sup> The floating chambers captured both ebullition and diffusive gas emissions and the  $k$  values provide insight into the relative importance of these emission mechanisms. Piston velocities calculated from  $\text{CO}_2$  ( $k_{600\text{-CO}_2}$ ; median =  $4.2 \text{ cm hr}^{-1}$ , Figure 2B) were consistent with values previously reported for diffusive emissions,<sup>4,15</sup> suggesting that diffusion was the dominant  $\text{CO}_2$  emission pathway and that the floating chambers did not artificially enhance emissions by disturbing the air–water interface.<sup>34</sup> Some  $\text{CH}_4$  piston velocities ( $k_{600\text{-CH}_4}$ ; median =  $27.2 \text{ cm hr}^{-1}$ , Figure 2A) were too large to be attributed strictly to diffusion and were likely enhanced by surfacing  $\text{CH}_4$ -rich bubbles. The ratio of  $k_{600\text{-CH}_4}$  and  $k_{600\text{-CO}_2}$  (median = 21) was greatest at the two shallowest sites (UP and EN), suggesting that bubble ebullition was greatest at those sites. The magnitude of the difference between  $k_{600\text{-CH}_4}$  and  $k_{600\text{-CO}_2}$  was too large to be attributed to surfacing microbubbles, which can enhance  $\text{CH}_4$  gas transfer by  $5\text{--}9 \text{ cm hr}^{-1}$ ,<sup>15,35</sup> and is likely the result of  $\text{CH}_4$ -rich macrobubbles.

Another explanation for the high  $\text{CH}_4$  emissions from the river delta is that sediment  $\text{CH}_4$  production at UP was greater than at the other sites. This is consistent with our finding that  $\text{CH}_4$  emissions from the UP site were on average ca. 2.7 times greater (median = 1.6) than rates of  $\text{CH}_4$  production at OF, the most downstream and deepest site, possibly because high loadings and rapid burial of organic matter in river deltas fosters high rates of sediment  $\text{CH}_4$  production, as described in the “deltaic zone” hypothesis.<sup>36</sup> This may be particularly important in reservoirs draining agricultural basins which often have high rates of soil erosion and subsequent sediment loading to receiving waters.<sup>37</sup> During an additional survey of  $\text{CH}_4$  emissions near tributaries in Harsha Lake (data reported alongside site locations in Figure 1), none of the other delta sites had rates as high as UP, possibly because the other tributaries drained much smaller basins ( $60\text{--}80 \text{ km}^2$ ) with a lower intensity of agricultural activity. However, the rates were generally 6 times greater than the mid reservoir site (EN), providing additional evidence that river deltas have higher  $\text{CH}_4$  emissions than open waters. The UP site also had higher overall respiration rates than the other sites, as



indicated by higher total carbon emissions ( $\text{CH}_4 + \text{CO}_2$ ), which is consistent with the notion that the quantity or quality of sediment C was greater at the river delta site.

#### Comparison to Other Published $\text{CH}_4$ Emission Rates.

After accounting for spatial and temporal variability, we estimated an annual reservoir-wide emission rate of  $176 \pm 36 \text{ mg C m}^{-2} \text{ d}^{-1}$ . This value is within the range of estimates from tropical systems ( $101\text{--}1471 \text{ mg C m}^{-2} \text{ d}^{-1}$ ), but up to 3 orders of magnitude higher than most reports from temperate systems ( $<1\text{--}50 \text{ mg C m}^{-2} \text{ d}^{-1}$ ).<sup>6</sup> The exceptions to this pattern include a temperate reservoir in Switzerland<sup>38</sup> ( $117 \text{ mg C m}^{-2} \text{ d}^{-1}$ ) and a small river impoundment ( $0.38 \text{ km}^2$ ) in Germany<sup>8</sup> ( $333 \text{ mg C m}^{-2} \text{ d}^{-1}$ ), where high emissions were largely attributed to extreme ebullition rates. One reason the rates reported here are relatively high may be that we accounted for emissions from the main river delta, while most of the literature data represent emissions from the surface of deeper areas of reservoirs, which, based on our findings, likely underestimates reservoir-wide emissions.<sup>6</sup> Even when excluding UP from the data set, however, the mean  $\text{CH}_4$  emission rate ( $85 \pm 26 \text{ mg C m}^{-2} \text{ d}^{-1}$ ) is still higher than estimates from most other midlatitude reservoirs, likely because high nutrient loading, sedimentation, and persistent algae blooms in Harsha Lake have stimulated methanogenesis.<sup>39</sup> It is worth noting that our estimate likely represents a lower bound for the true rate because we did not quantify ebullition hot spots<sup>38</sup> or enhanced night-time emissions that can occur during periods of convective mixing.<sup>32</sup> It is unclear whether our results can be generalized to other midlatitude agricultural impacted reservoirs. Eagle Creek Reservoir (ECR), an agricultural impacted reservoir about 160 km from Harsha Lake, is also subject to high nutrient and sediment loading, yet supports an annual  $\text{CH}_4$  emission rate only  $\sim 5\%$  ( $10 \text{ mg C m}^{-2} \text{ d}^{-1}$ )<sup>7</sup> of that at Harsha Lake. The ECR study did not include river deltas, but even after excluding the Harsha Lake river delta site from the comparison,  $\text{CH}_4$  emission rates from Harsha were 8.5 times greater than that at ECR ( $85$  vs  $10 \text{ mg C m}^{-2} \text{ d}^{-1}$ ). Another factor complicating the comparison is that emissions at ECR were estimated using a wind based model while emissions were directly measured at Harsha Lake. Whether Harsha Lake or ECR represents the typical midlatitude agricultural reservoir is unknown, but this question has strong implications for our understanding of the global  $\text{CH}_4$  budget. We estimate there are ca.  $35\,000 \text{ km}^2$  of reservoirs draining corn and soybean croplands, the dominant crops in the Harsha Lake watershed, in the United States. Combining this surface area estimate with the annual emission rate measured at Harsha Lake, results in an estimate of annual  $\text{CH}_4$  emissions from agricultural impacted reservoirs in the United States of  $2.2 \text{ Tg C}$ . This represents potential reservoir  $\text{CH}_4$  emissions not accounted for in current inventories and is equivalent to 60% of annual  $\text{CH}_4$  emissions from all the landfills in the United States ( $3.7 \text{ Tg CH}_4\text{-C yr}^{-1}$ ) or about 10% of the nation's annual anthropogenic  $\text{CH}_4$  emissions.<sup>40</sup> This estimate should be viewed with caution, however, because it is based on  $\text{CH}_4$  emission rate measurements made at only one lake and does not account for numerous variables that could control reservoir  $\text{CH}_4$  emissions including the number and size of river deltas in each reservoir.

#### Greenhouse Gas Emissions Mitigation Strategies.

Previous studies have shown that degassing while water is routed through the dam is a major source of  $\text{CH}_4$  emissions from reservoirs, comprising up to 33% of total reservoir emissions.<sup>41,42</sup> We estimate that this pathway constitutes only

0.8% of annual  $\text{CH}_4$  emissions from Harsha Lake. In Harsha Lake, summer time water withdrawals are largely restricted to shallow depths to protect the dam from corrosive hydrogen sulfide gas and to maintain acceptably high dissolved oxygen in the receiving waters. Consequently, the highly  $\text{CH}_4$  supersaturated water in the hypolimnion does not pass through the dam. If water at Harsha Lake were exclusively withdrawn from the hypolimnion, then we estimate that dam degassing would comprise 23–28% of annual  $\text{CH}_4$  emissions, assuming that diffusive emissions would be unaffected. Therefore, an important engineering strategy for minimizing  $\text{CH}_4$  emissions from reservoirs is to allow for the withdrawal of shallow waters during periods of thermal stratification.

Minimizing the surface area of the river delta through water level management may also reduce overall  $\text{CH}_4$  emissions from reservoirs. While the river delta near the UP site comprised a small proportion of the reservoir surface area (i.e., 3–8%, depending on pool elevation), it was the source of 64% of reservoir  $\text{CH}_4$  emissions on average (Figure 1, 5A) and should therefore be the focus of  $\text{CH}_4$  mitigation actions. Most suggested management actions are long-term and include reducing watershed soil erosion<sup>38</sup> and nutrient exports.<sup>9</sup> While these approaches are the best long-term solution, there is a need for mitigation efforts that have a more immediate effect. We estimate that lowering the target pool elevation during the summer by 2 m would reduce the reservoir surface area by  $1.2 \text{ km}^2$ , much of which is located in the river delta areas (Figure 1), resulting in up to a 35% reduction in reservoir wide  $\text{CH}_4$  emissions, assuming that the newly exposed soils do not emit  $\text{CH}_4$ . The long-term efficacy of this approach is unclear, however, because the  $\text{CH}_4$  emission hot-spot may shift downriver to the site of active sediment deposition established under the lower pool elevation. Another possibility is to periodically dredge river deltas to remove methanogenic sediments and increase water depth, although this process is energy-intensive and will lead to increased anthropogenic  $\text{CO}_2$  emissions. While these approaches are untested, they highlight a need for new research that yields actionable mitigation plans that federal and state agencies can use to reduce the greenhouse gas footprint of reservoirs, as encouraged by the White House's 2013 Executive Order.<sup>43</sup>

**Future Directions.** This study demonstrates that midlatitude agricultural reservoirs have  $\text{CH}_4$  emission rates comparable to those observed in the tropics, and intrareservoir variation in emission rates can be extreme. To improve the accuracy of national and global estimates of reservoir  $\text{CH}_4$  emissions it is critical that future studies account for emission hotspots within reservoirs. Furthermore, future work should focus on relatively understudied midlatitude agricultural impacted reservoirs, which may comprise a much larger component of the anthropogenic  $\text{CH}_4$  budget than currently recognized.

## ■ ASSOCIATED CONTENT

### 📄 Supporting Information

An extended methods section, five additional figures, and two tables. This material is available free of charge via the Internet at <http://pubs.acs.org/>.

## ■ AUTHOR INFORMATION

### Corresponding Author

\*beaulieu.jake@epa.gov.

## Present Address

#URS Corporation, Cincinnati, Ohio 45202.

## Notes

The authors declare no competing financial interest.

## ACKNOWLEDGMENTS

We thank Jade Young and Jim O'Boyle of the U.S. Army Corp of Engineers for logistical support. We also thank Kit Daniels, Dana Macke, Eric Kleiner, and Don Brown for field and lab assistance. The U.S. Environmental Protection Agency, through its Office of Research and Development funded and managed this research. It has been subjected to the Agency's administrative review and has been approved for external publication. Any opinions expressed in this paper are those of the authors and do not necessarily reflect the views of the Agency, therefore, no official endorsement should be inferred. Any mention of trade names or commercial products does not constitute endorsement or recommendation for use.

## REFERENCES

- (1) Myhre, G.; Shindell, D.; Bréon, F.-M.; Collins, W.; Fuglestedt, J.; Huang, J.; Koch, D.; Lamarque, J.-F.; Lee, D.; Mendoza, B.; Nakajima, T.; Robock, A.; Stephens, G.; Takemura, T.; Zhang, H., Anthropogenic and natural radiative forcing. In *Climate Change 2013: The Physical Science Basis. Contribution of Working Group I to the Fifth Assessment Report of the Intergovernmental Panel on Climate Change*; Stocker, T. F., Qin, D., Plattner, G.-K., Tignor, M., Allen, S. K., Boschung, J., Nauels, A., Bex, V., Midgely, P. M., Eds.; Cambridge University Press: Cambridge, U.K. and New York, U.S.A., 2013.
- (2) Townsend-Small, A.; Tyler, S. C.; Pataki, D. E.; Xu, X. M.; Christensen, L. E. Isotopic measurements of atmospheric methane in Los Angeles, influence of "fugitive" fossil fuel emissions, California, U.S.A. *J. Geophys. Res.-Atmos.* **2012**, *117*.
- (3) Miller, S. M.; Wofsy, S. C.; Michalak, A. M.; Kort, E. A.; Andrews, A. E.; Biraud, S. C.; Dlugokencky, E. J.; Eluszkiewicz, J.; Fischer, M. L.; Janssens-Maenhout, G.; Miller, B. R.; Miller, J. B.; Montzka, S. A.; Nehrkorn, T.; Sweeney, C. Anthropogenic emissions of methane in the United States. *Proc. Natl. Acad. Sci. U. S. A.*, **2013**.
- (4) Bastviken, D.; Cole, J. J.; Pace, M. L.; Van de Bogert, M. C. Fates of methane from different lake habitats: Connecting whole-lake budgets and CH<sub>4</sub> emissions. *J. Geophys. Res.-Biogeosci.* **2008**, *113*, G2.
- (5) St. Louis, V. L.; Kelly, C. A.; Duchemin, É.; Rudd, J. W. M.; Rosenberg, D. M. Reservoir surfaces as sources of greenhouse gases to the atmosphere: A global estimate. *Bioscience* **2000**, *50* (9), 766–775.
- (6) Barros, N.; Cole, J. J.; Tranvik, L. J.; Prairie, Y. T.; Bastviken, D.; Huszar, V. L. M.; del Giorgio, P.; Roland, F. Carbon emission from hydroelectric reservoirs linked to reservoir age and latitude. *Nat. Geosci.* **2011**, *4* (9), 593–596.
- (7) Jacinthe, P. A.; Filippelli, G. M.; Tedesco, L. P.; Raftis, R. Carbon storage and greenhouse gases emission from a fluvial reservoir in an agricultural landscape. *CATENA* **2012**, *94* (0), 53–63.
- (8) Maeck, A.; DelSontro, T.; McGinnis, D. F.; Fischer, H.; Flury, S.; Schmidt, M.; Fietzek, P.; Lorke, A. Sediment trapping by dams creates methane emission hot spots. *Environ. Sci. Technol.* **2013**, *47* (15), 8130–8137.
- (9) West, W. E.; Coloso, J. J.; Jones, S. E. Effects of algal and terrestrial carbon on methane production rates and methanogen community structure in a temperate lake sediment. *Freshw. Biol.* **2012**, *57* (5), 949–955.
- (10) Ioffe, B. V.; Vitenberg, A. G. *Head-Space Analysis and Related Methods in Gas Chromatography*; Wiley: New York, 1984.
- (11) Weiss, R. F. Carbon dioxide in water and seawater: the solubility of a non-ideal gas. *Mar. Chem.* **1974**, *2* (3), 203–215.
- (12) Yamamoto, S.; Alcauskas, J. B.; Crozier, T. E. Solubility of methane in distilled water and seawater. *J. Chem. Eng. Data* **1976**, *21* (1), 78–80.
- (13) Tans, P.; Keeling, R. ESRL/GMD FTP data finder. <http://www.esrl.noaa.gov/gmd/dv/data/> (11/05/2013).
- (14) Yarnes, C.  $\delta^{13}\text{C}$  and  $\delta^2\text{H}$  measurement of methane from ecological and geological sources by gas chromatography/combustion/pyrolysis isotope-ratio mass spectrometry. *Rapid Commun. Mass Spectrom.* **2013**, *27* (9), 1036–1044.
- (15) Beaulieu, J. J.; Shuster, W. D.; Rebholz, J. A. Controls on gas transfer velocities in a large river. *J. Geophys. Res.* **2012**, *117* (G2), G02007.
- (16) United States Army Corps of Engineers National Inventory of Dams. <http://geo.usace.army.mil/pgis/f?p=397:1:0>.
- (17) United States Department of Agriculture Quick Stats 2.0. [http://www.nass.usda.gov/Quick\\_Stats/](http://www.nass.usda.gov/Quick_Stats/).
- (18) Beaulieu, J. J.; Smolenski, R. L.; Nietch, C. T.; Townsend-Small, A.; Elovitz, M. S.; Schubauer-Berigan, J. P. Denitrification alternates between a source and sink of nitrous oxide in the hypolimnion of a thermally stratified reservoir. *Limnol. Oceanogr.* **2014**, *59* (2), 495–506.
- (19) Happell, J. D.; Chanton, J. P.; Showers, W. S. The influence of methane oxidation on the stable isotopic composition of methane emitted from Florida swamp forests. *Geochim. Cosmochim. Acta* **1994**, *58* (20), 4377–4388.
- (20) Bastviken, D.; Ejlertsson, J.; Tranvik, L. Measurement of methane oxidation in lakes: A comparison of methods. *Environ. Sci. Technol.* **2002**, *36* (15), 3354–61.
- (21) Kankaala, P.; Huotari, J.; Peltomaa, E.; Saloranta, T.; Ojala, A. Methanotrophic activity in relation to methane efflux and total heterotrophic bacterial production in a stratified, humic, boreal lake. *Limnol. Oceanogr.* **2006**, *51* (2), 1195–1204.
- (22) Zuur, A. F.; Ieno, E. N.; Walker, N. J.; Saveliev, A. A.; Smith, G. M. *Mixed Effects Models and Extensions in Ecology with R*; Springer: New York, NY, 2009.
- (23) Sakamoto, Y.; Ishiguro, M.; Kitagawa, G. *Akaike Information Criterion Statistics*; Reidel Publishing Company: Netherlands, 1986.
- (24) R Development Core Team. R: A Language and Environment for Statistical Computing. <http://www.R-project.org>.
- (25) Pinheiro, J.; Bates, D.; DebRoy, S.; Sarkar, D. R Development Core Team. nlme: Linear and Nonlinear Mixed Effects Models. R package version 3.1–113. 2011.
- (26) Hothorn, T.; Bretz, F.; Westfall, P. Simultaneous inference in general parametric models. *Biomet. J.* **2008**, *50* (3), 346–363.
- (27) Kelly, C. A.; Chynoweth, D. P. The contributions of temperature and of the input of organic matter in controlling rates of sediment methanogenesis. *Limnol. Oceanogr.* **1981**, *26* (5), 891–897.
- (28) Ojala, A.; Bellido, J. L.; Tulonen, T.; Kankaala, P.; Huotari, J. Carbon gas fluxes from a brown-water and a clear-water lake in the boreal zone during a summer with extreme rain events. *Limnol. Oceanogr.* **2011**, *56* (1), 61–76.
- (29) Hofmann, H. Spatiotemporal distribution patterns of dissolved methane in lakes: How accurate are the current estimations of the diffusive flux path? *Geophys. Res. Lett.* **2013**, *40* (11), 2779–2784.
- (30) Grossart, H. P.; Frindte, K.; Dziallas, C.; Eckert, W.; Tang, K. W. Microbial methane production in oxygenated water column of an oligotrophic lake. *Proc. Natl. Acad. Sci. U. S. A.* **2011**, *108* (49), 19657–61.
- (31) Schubert, C. J.; Diem, T.; Eugster, W. Methane emissions from a small wind shielded lake determined by eddy covariance, flux chambers, anchored funnels, and boundary model calculations: A comparison. *Environ. Sci. Technol.* **2012**, *46* (8), 4515–4522.
- (32) Podgrajsek, E.; Sahlee, E.; Rutgersson, A. Diurnal cycle of lake methane flux. *J. Geophys. Res.-Biogeosci.* **2014**, *119* (3), 236–248.
- (33) McGinnis, D. F.; Greinert, J.; Artemov, Y.; Beaubien, S. E.; Wüest, A. Fate of rising methane bubbles in stratified waters: How much methane reaches the atmosphere? *J. Geophys. Res.* **2006**, *111* (C9), C09007.
- (34) Matthews, C. J. D.; St; Louis, V. L.; Hesslein, R. H. Comparison of three techniques used to measure diffusive gas exchange from



sheltered aquatic surfaces. *Environ. Sci. Technol.* **2003**, *37* (4), 772–780.

(35) Prairie, Y. T.; del Giorgio, P. A. A new pathway of freshwater methane emissions and the putative importance of microbubbles. *Inland Waters* **2013**, *3* (3), 311–320.

(36) DelSontro, T.; Kunz, M. J.; Kempter, T.; Wuest, A.; Wehrli, B.; Senn, D. B. Spatial heterogeneity of methane ebullition in a large tropical reservoir. *Environ. Sci. Technol.* **2011**, *45* (23), 9866–9873.

(37) Heathcote, A. J.; Downing, J. A. Impacts of eutrophication on carbon burial in freshwater lakes in an intensively agricultural landscape. *Ecosystems* **2012**, *15* (1), 60–70.

(38) Delsontro, T.; McGinnis, D. F.; Sobek, S.; Ostrovsky, I.; Wehrli, B. Extreme methane emissions from a swiss hydropower reservoir: Contribution from bubbling sediments. *Environ. Sci. Technol.* **2010**, *44* (7), 2419–2425.

(39) Hulthe, G.; Hulth, S.; Hall, P. O. J. Effect of oxygen on degradation rate of refractory and labile organic matter in continental margin sediments. *Geochim. Cosmochim. Acta* **1998**, *62* (8), 1319–1328.

(40) U.S. Environmental Protection Agency. *Inventory of U.S. Greenhouse Gas Emissions and Sinks: 1990–2011*, 2013.

(41) Guérin, F.; Abril, G.; Richard, S.; Burban, B.; Reynouard, C.; Seyler, P.; Delmas, R., Methane and carbon dioxide emissions from tropical reservoirs: Significance of downstream rivers. *Geophys. Res. Lett.* **2006**, *33*, (21).

(42) Galy-Lacaux, C.; Delmas, R.; Jambert, C.; Dumestre, J.-F.; Labroue, L.; Richard, S.; Gosse, P. Gaseous emissions and oxygen consumption in hydroelectric dams: A case study in French Guyana. *Global Biogeochem. Cycles* **1997**, *11* (4), 471–483.

(43) Obama, B. *Executive Order—Preparing the United States for the Impacts of Climate Change*. <http://www.whitehouse.gov/the-press-office/2013/11/01/executive-order-preparing-united-states-impacts-climate-change> (7/3/2014).